

Review

The Importance of Laminae for China Lacustrine Shale Oil Enrichment: A Review

Shang Xu ¹ and Qiyang Gou ^{2,*}¹ School of Geosciences, China University of Petroleum, Qingdao 266580, China² Key Laboratory of Tectonics and Petroleum Resources, Ministry of Education, China University of Geosciences, Wuhan 430074, China

* Correspondence: gouqiyang0709@cug.edu.cn

Abstract: The laminar structure of shale system has an important influence on the evaluation of hydrocarbon source rock quality, reservoir quality, and engineering quality, and it is receiving increasing attention. A systematic study of the lamina structure is not only of great scientific significance but also of vital practical importance for shale oil production. In this paper, the identification and description classification of shale laminae are first reviewed. Multiple scales and types indicate that a combination of different probe techniques is the basis for an accurate evaluation of shale laminar characteristics. The influence of laminae on shale reservoir, oil-bearing, mobility, and fracability properties is discussed systematically. A comparative analysis shows that shale systems with well-developed lamination facilitate the development of bedding fractures, thus improving the shale storage space. The average pore size and pore connectivity are also enhanced. These factors synergistically control the superior retention and flow capacity of shale oil in laminated shales. In such conditions, the high production of shale oil wells can still be achieved even if complex networks of fracturing cracks are difficult to form in shale systems with well-developed lamination. This work is helpful to reveal the enrichment mechanism of shale oil and clarify the high-yield law of hydrocarbons, so as to guide the selection of sweet spots.

Keywords: shale oil; lamina structure; enrichment mechanism; movable oil; fracability



Citation: Xu, S.; Gou, Q. The Importance of Laminae for China Lacustrine Shale Oil Enrichment: A Review. *Energies* **2023**, *16*, 1661. <https://doi.org/10.3390/en16041661>

Academic Editor: Reza Rezaee

Received: 20 December 2022

Revised: 14 January 2023

Accepted: 1 February 2023

Published: 7 February 2023



Copyright: © 2023 by the authors. Licensee MDPI, Basel, Switzerland. This article is an open access article distributed under the terms and conditions of the Creative Commons Attribution (CC BY) license (<https://creativecommons.org/licenses/by/4.0/>).

1. Introduction

Compared to conventional petroleum systems, shale strata exhibit the characteristics of extremely low porosity and ultralow permeability. However, the development of horizontal drilling and multistage hydraulic fracturing technologies has allowed the commercial extraction of hydrocarbons from tight shale deposits that were unprofitable decades ago [1–6]. In North America, drilling in the Bakken shale and the Eagle Ford shale confirmed the availability of hydrocarbon liquid resources [1]. The shale oil production in the United States reached an annual level of 2.349 billion barrels in 2018, accounting for 64.7% of the total oil production. This value is expected to reach 9.46 million barrels per day in 2040, accounting for 67.3% of the total US oil production [7–10]. Following in the footsteps of the US, China is also aggressively examining its unconventional resource potential targeting shale oil plays [1,8,9]. Large-scale shale oil exploration in diverse petroliferous basins, e.g., Junggar Basin, Ordos Basin, Jiangnan Basin, Bohai Bay Basin, and Songliao Basin, has revealed that China contains abundant shale oil resources [7–12]. The estimated total mass of the technically recoverable resources of shale oil in China is between 7.4×10^9 and 3.7×10^{10} t [7,12]. Currently, an annual shale oil production of about 160×10^4 t has been realized, which makes it possible for shale oil to provide new opportunities for strengthening the energy security of China [8,10,12].

Compared to the North America, the petroleum in China is mostly extracted from lacustrine shale instead of marine shale [8,9,13]. It is worth noting that lake basin sedimentary phases are diverse, with small sedimentation scales and shallow water depth, and they

are more influenced by paleoclimatic changes [1,14,15]. Hence, it is easy to form a variety of laminar structures in lacustrine shale systems [16–22]. More importantly, the expansion of works has realized that laminated shales usually have high total organic carbon (TOC) content and superior reservoir quality. Exploration practice from the Shengli Geophysical Research Institute of Sinopec has shown that shale oil produced by conventional measures mainly comes from laminated shales. Statistics on shale oil-producing wells (more than 300 wells) in the Jiyang Depression indicate that laminated shales with industrial oil flows account for approximately 70% of total pay intervals [15,22]. In other words, the laminated structure is also closely related to oil production [11,21–23]. With these results, it is urgent to understand the development characteristics of shale laminae and systematically summarize its impact on oil molecule accumulation, so as to realize commercial production of continental shale oil in China.

Starting from the identification of laminae in shale reservoirs, this paper first summarizes the current common division schemes of lamina types. After that, the effects of laminae structure on shale reservoir, oil-bearing, and mobility properties are discussed. Furthermore, the relationship between laminae and shale fracability is preliminarily analyzed. In general terms, this work is helpful to reveal the enrichment and high-yield mechanism of hydrocarbons from tight unconventional reservoirs.

2. Identification of Multiscale Laminae

The lamina is the smallest megascopic layer without internal layers in fine-grained sedimentary rocks [24,25]. The thickness is generally less than 1 cm [11,26,27]. The mineral composition within a single lamina is relatively uniform [27]. Generally, laminae are interpreted to form in response to small-scale fluctuations within a single flow or depositional event in the rates of the controlling processes, e.g., seasonal growth of planktic or benthic organisms [11,15]. In addition, some laminae may be associated with late diagenetic transformation, such as coarse-grained calcite laminae, which is widely observed in the Shahejie Formation shale in the Dongying sag [16,22]. In such cases, the lamina may have multiscale characteristics in different observational settings. Lamellar features ranging from macroscopic (meter scale) to microscopic (mm to μm scale) have been extensively reported by previous studies [11,17,25,28–30] (Figure 1). In general, the meter and centimeter lamina structures reflect variations of vertical superposition lithology, while millimeter and micrometer lamina structures reflect mineral superimposition patterns [31,32].

Core observation can directly depict the centimeter- to millimeter-scale laminae, as well as obtain various superposition methods of different mineral compositions on this scale [27,29] (Figure 1B). The submillimeter- to micron-scale lamellar structures can be further quantitatively described by using thin sections and scanning electron microscopy (SEM) (Figure 1C,D). However, core and microscopic data are limited and often discontinuous, making it difficult to effectively predict the vertical distribution of laminae in a whole well [30,33]. Conversely, well-log data, e.g., a series of conventional logs and image logs, offer special advantages for continuous evaluation [25,30,34]. In particular, image logging has been applied to the identification of laminae on the subcentimeter scale because of its high vertical resolution ($\sim 5\text{mm}$) (Figure 1A). For example, Wang et al. [30] and Pang et al. [25] offered the characteristics of shale multiscale laminae of Fengcheng Formation in Mahu Sag and Lucaogou Formation in Jimusar Sag through imaging logging, respectively, which provided insights for the prediction of sweet spots in the study area. It should be noted that the resolution of the image tool is limited (the vertical resolution is usually 5 mm), which can lead to the loss of microscopic lamina information [30,34]. In other words, the laminated structure investigated by imaging logs is strictly more of a laminar combination, which may contain a large number of basic laminae on the μm scale. Overall, the joint use of multiple methods is the key to the effective evaluation of multiscale laminae (Figure 1).

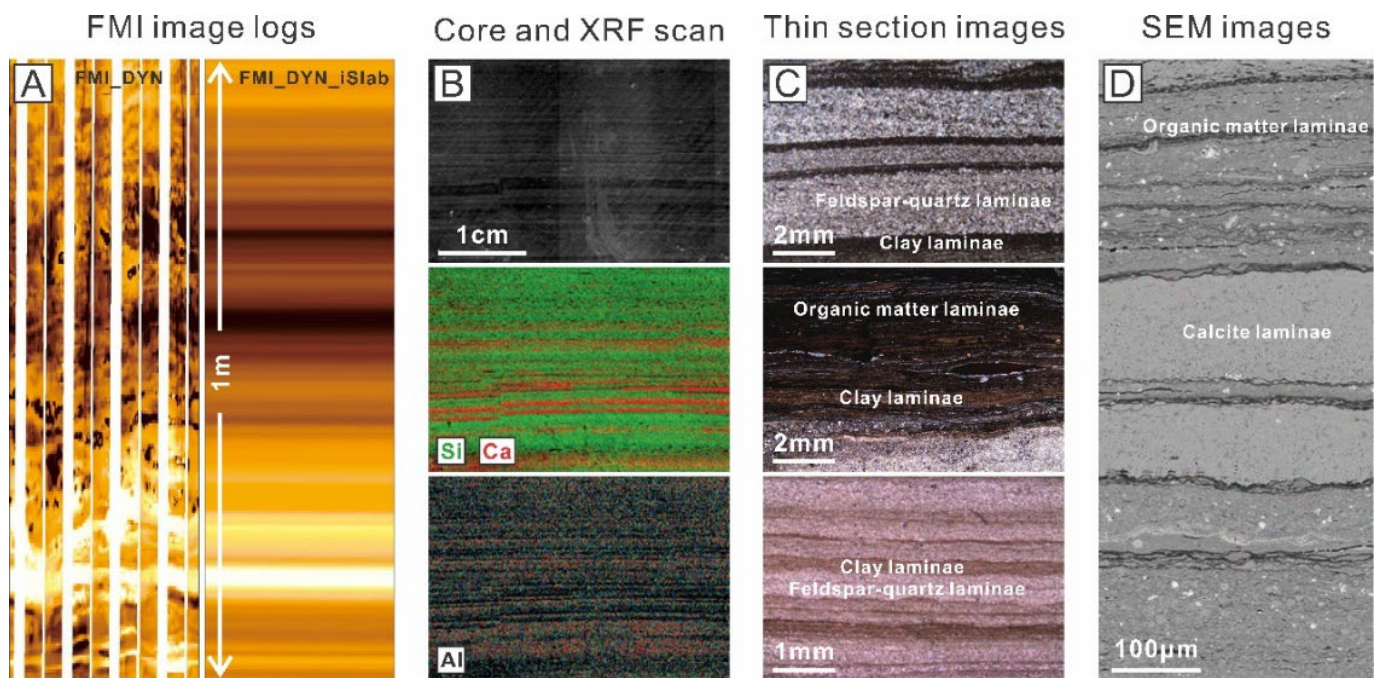


Figure 1. The identification of multiscale laminae in shale reservoir based on the combination of multiple methods, modified after Pang et al. [25], Xu et al. [20], Wu et al. [11], and Wang et al. [18]. (A) Laminae structure and their characteristics on FMI image logs. (B) The recognition of laminae on core images and XRF scan. (C) Various laminated types represented by thin section images. (D) Various laminated types represented by SEM images.

3. Descriptive Classification of Shale Laminae

Currently, a number of categories have been used to divide the shale laminae [27,29,30,35–38]. Among them, mineral composition is the most common basis for classification. In such cases, with the application of image observation, clay mineral lamination, felsic lamination, carbonate lamination, and organic matter lamination are widely recognized in the lacustrine shale systems of China (Figure 1) [20,21,38–40]. Furthermore, the parameters of lamina, e.g., continuity, shape, and geometry, are used to capture lamination (Figure 2). With these results, three major categories and 12 subclasses of laminae are proposed [35,37], and common lamination patterns and their corresponding images are shown in Figure 2. In addition, Shi et al. [22] divided laminae into thin parallel laminae, thick parallel laminae, wavy laminae, lenticular laminae, sandy laminae, and weak laminae according to the laminar shapes and structures. Moreover, Dong et al. [41] determined the thickness of bedding through core observation and thin section identification, classifying laminar spacing >50 cm as massive, 10–50 cm as layered, 1–10 cm as thin laminae, 1 mm–1 cm as laminae, and <1 mm as sheet. The demarcation point between laminae and layers, according to Liu et al. [27], was set at 1 mm (laminae < 1 mm, layer ≥ 1 mm). Similarly, the value of 1 cm to distinguish lamina and layered structure was implemented in the work of Pang et al. [25]. The aforementioned discussion indicates that the laminae have gradually undergone a transformation in terms of classification and characterization from a single feature to a comprehensive feature [17,42,43]. Laminae can no longer be accurately described solely by virtue of their thickness, shape, and mineral composition.

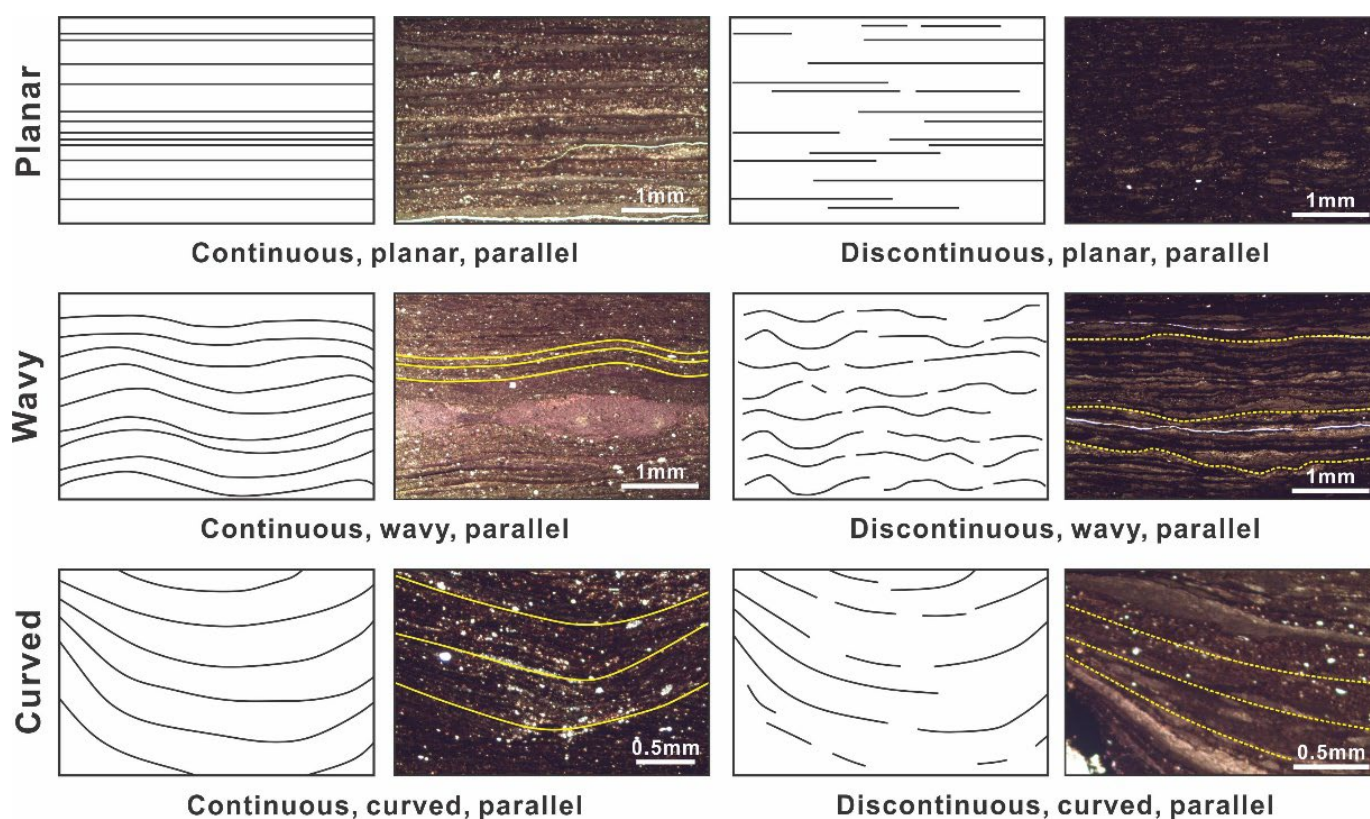


Figure 2. Descriptive terms for lamina continuity, shape, and geometry, modified after Lazar et al. [37] and Campbell [35]. Solid yellow lines indicate continuous laminae, and dashed yellow lines indicate discontinuous laminae.

4. The Role of Laminae for Shale Oil Enrichment and High Yield

4.1. Control of Laminae on Reservoir Property

The occurrence states of oil molecules in shale reservoirs including free oil occurs in pores and microfractures, adsorbed oil storage in kerogen and on the mineral particle surface, and a small amount of oil that dissolves in the kerogen [44–47]. The work of Chen et al. [48] pointed out that about 80% of shale oil is distributed in macropores of shale reservoir. Hence, the pore structure, including pore size, pore volume, and porosity, possesses an important influence on shale oil storage capacity [49–53]. In addition, previous studies have indicated that the contact boundary between various laminae belongs to the mechanically weak surface of shale rock, which easily forms laminar fractures during geological evolution, thus improving the reservoir's physical properties [8,9,12,54–56]. For example, using NMR and helium porosity tests, Wang et al. [57] and Ning et al. [58] systematically compared shales with different structures in Dongying Sag. Their works pointed out that laminar shales have higher porosity and permeability, followed by layer shales, with massive shales having the lowest (Figure 3A–C). Similar conclusions were demonstrated in [38,59–66]. In particular, based on the quantitative detection of high pressure mercury injection, Bao [60] and Zhang et al. [61] further proposed that the porosity of lamellar shale is mainly provided by pores with a size of 10–30 nm, and the contribution rate is about 32.6–55.2%. Meanwhile, pores with a size of more than 100 nm also have a certain contribution. However, the porosity of massive shale is mainly provided by pores smaller than 10 nm, which generally account for 57.96–99.64% of the total effective pores, with an average value of 78.14%. More importantly, no pores with a size larger than 100 nm could be observed in the massive samples [60,61]. It is worth noting that many studies have also found pores with a diameter of >100 nm in massive shale, but the number is obviously lower than that of laminated shale [57,59,62,67–71].

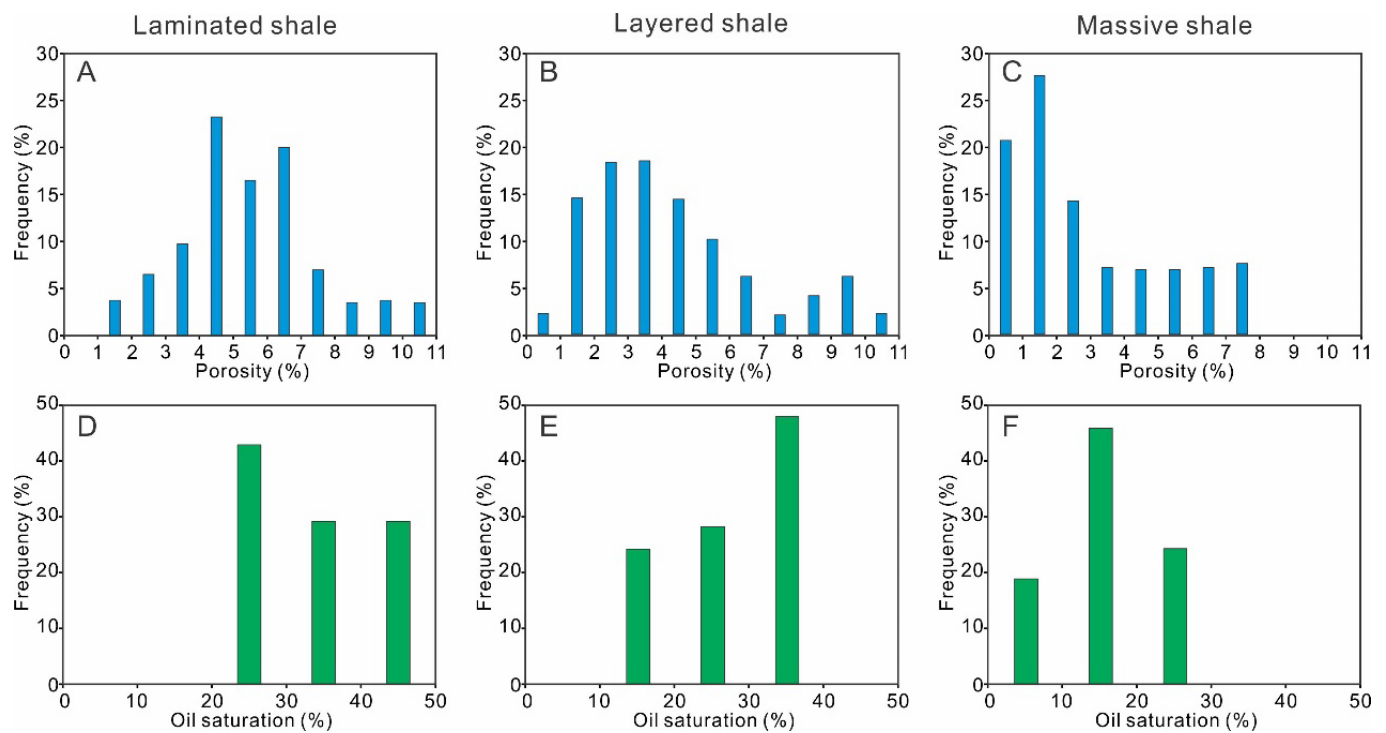


Figure 3. Frequency distribution of physical properties and oil saturation of different lamina structure, modified after Ning et al. [58]. (A) and (D) Frequency distribution of porosity and oil saturation of laminated shale. (B) and (E) Frequency distribution of porosity and oil saturation of layered shale. (C) and (F) Frequency distribution of porosity and oil saturation of massive shale.

According to the quantitative statistical results of SEM images, on the other hand, Liu et al. [68] and Zhang [72] identified that various pore types are developed in shales with different structures in the Shahejie Formation of Jiyang Depression (Figure 4). However, the development degree of these pore types is quite different. Among them, lamellar shale is dominated by micron and ultra-micron storage spaces, while massive shale is mainly composed of interlamellar pores and shrinkage pores on the mesopore scale. Pore connectivity is another important parameter to describe the shale reservoir properties [73,74]. Jiang et al. [71] compared the nuclear magnetic resonance and mercury intrusion data of shale, and they concluded that the pore connectivity is ordered as follows: laminated shale > layered shale > massive shale. The same phenomenon was presented using fluid tracer migration [63] and CT scanning [23].

Collectively, the development of laminae promotes the formation of laminar microfractures. In such cases, the pore size of the laminated shale is obviously improved. Moreover, the microfractures can connect the pores, further increasing the porosity and permeability of shale reservoirs [69,71,72]. It is worth noting that the types of laminae are varied (Figure 1). Laminae composed of different minerals also have significantly different characteristics of compaction resistance, which leads to different pore structures between laminae. For example, through quantitative statistics of SEM images of different laminae in the Kongdian Formation shale, Li et al. [24] comprehensively pointed out that the internal pore diameter of carbonate laminae is small due to mineral cementation. At the same time, compared to mixed laminae (mainly composed of clay minerals and siliceous minerals), the work of Xin et al. [21] demonstrated that siliceous laminae possessed superior average porosity and pore size. In addition, Wu et al. [11] found that the porosity and pore size were smaller because of the toughness of the clay laminae and organic matter laminae. As mentioned above, the development characteristics of laminae control the storage conditions of shale reservoirs, which is the basis for shale oil enrichment [47,49,59].

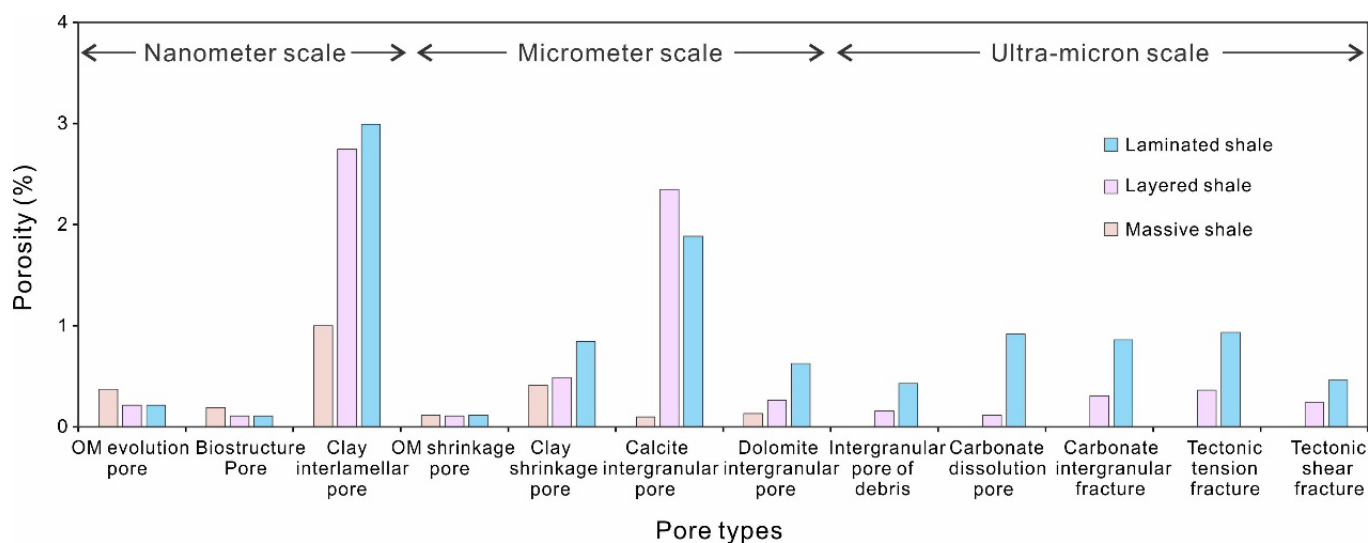


Figure 4. The main types of reservoir space contribute to the shale porosity for different lamina structure, modified after Zhang [72].

4.2. Influence of Laminae on Oil-Bearing Property

The oil-bearing property of shale refers to the hydrocarbon content retained in reservoirs [46,75]. Likewise, the retention behavior of oil molecules is closely related to the pore structure [46,76,77]. To sum up, from the above discussion, the increase in lamina development seems to be beneficial for the increase in shale oil content [11,53,58]. Ning et al. [58] analyzed Shahejie Formation shales in the Dongying Sag and reported more frequent laminae and a higher oil saturation in the shale. Specifically, the oil saturation of laminated shale is generally above 30%, while that of massive shale is less than 20% (Figure 3D–F). In particular, Shi et al. [22] further compared the difference in oil content in different lamina including thin parallel laminae, thick parallel laminae, wavy laminae, lenticular laminae, weak laminae, and sandy laminae. The first three types of laminae had good continuity and exhibited higher oil saturation values than the latter three types, which had poor laminar continuity. In addition, the free hydrocarbon content (S_1) based on Rock-Eval pyrolysis was also used to investigate the oil content in shales [11,20,57,78,79]. The evaluation results also revealed that the oil-bearing property was higher in laminated shale than that in massive shale [21,53,57]. In addition, the fluorescence characteristics are also important parameters to describe the occurrence and enrichment characteristics of shale oil [80,81]. Collectively, the observations of fluorescence thin sections under plane polarized light and fluorescence light show that the fluorescence in laminar shale samples is strong, and it is distributed linearly along the laminated plane or locally concentrated. However, the fluorescence in massive shale is dim and scattered in speckled features [75,82–84]. This phenomenon further proves that laminated shale has good oil-bearing properties.

In reality, the laminae can also affect the shale oil content by controlling the expulsion and retention of petroleum [70,82,84]. Generally, the contact surface between different types of laminae is the weak zone in the rock with the lowest rupture strength [58,69]. During the process of hydrocarbon generation and pressurization, these contact surfaces form a large number of microfractures, which promote oil discharge along the microfractures [13,29,47]. In particular, hydrocarbon generation simulation experiments have revealed that under the same or similar conditions, laminated shale has greater oil generation capacity (Figure 5) [85–87]. In such cases, the development degree of microfractures and the efficiency of hydrocarbon expulsion in lamellar shales can be further improved [47,57,82]. However, the well-developed laminated fractures can also significantly improve the pore structure and provide important reservoir space for oil storage in a shale system (Figures 3 and 4). Even though a large amount of shale oil may be expelled, as a result, the considerable storage space and oil generation capacity of laminated shale also

ensure the demand for shale oil enrichment [88,89]. For this reason, the oil-bearing property of laminated shale is still superior under the background of higher oil discharge efficiency (Figure 5). Overall, the laminar structure affects the hydrocarbon generation and expulsion process of shale oil, thus controlling the oil-bearing characteristics.

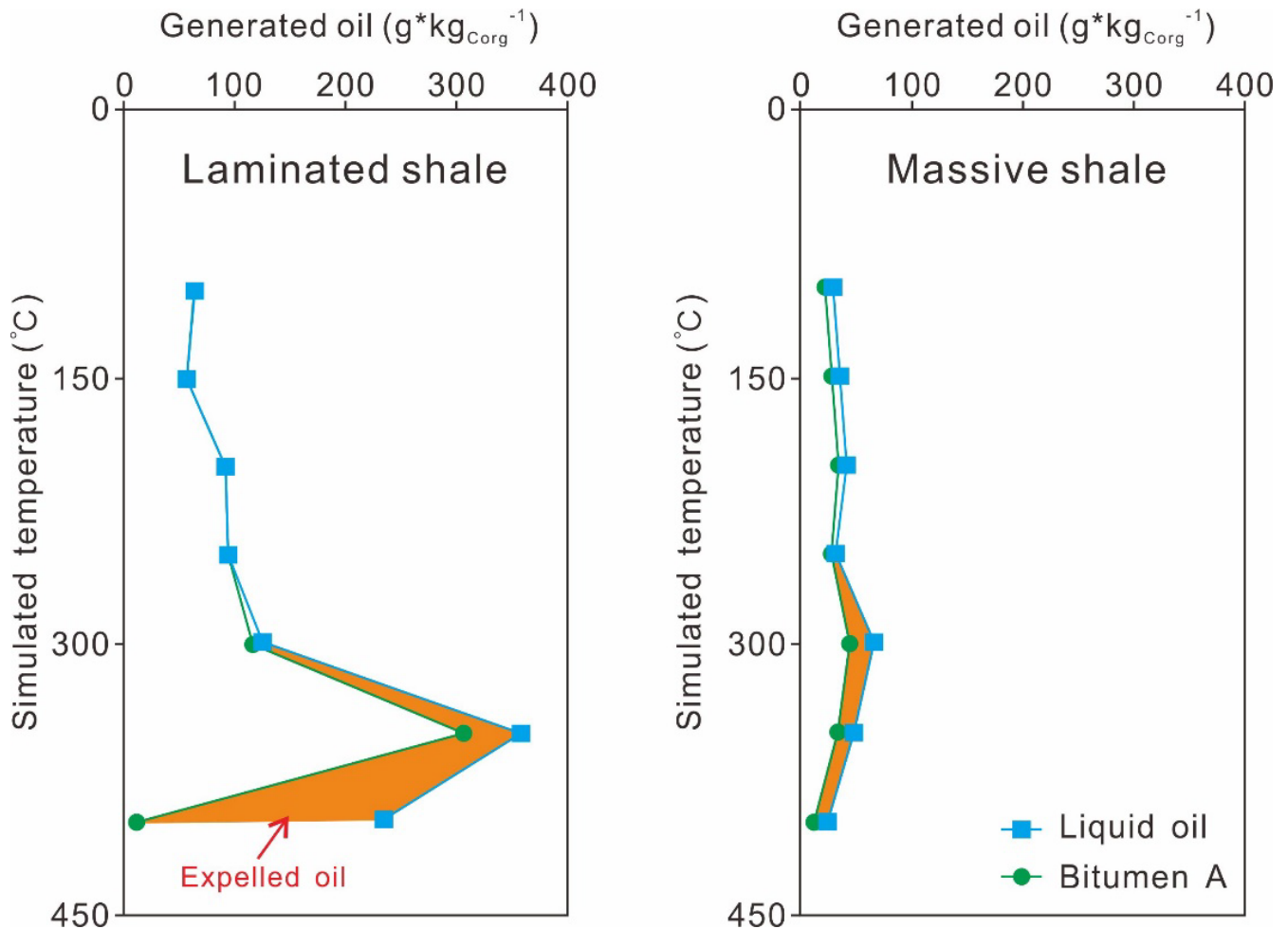


Figure 5. Ratio of generated and expelled oil of different laminar structure shales with simulated temperature, modified after Zhang et al. [86]. The TOC, Ro, and kerogen type of laminated shale are 3.2%, 0.42%, and type I, respectively, while those of massive shale are 2.05%, 0.42%, and type II₁, respectively.

4.3. Effect of Laminae on Shale Oil Mobility

The mobility of petroleum in shales is the key to the high yield of shale oil wells [44,58,90–92]. On the one hand, the mobility of shale oil depends on the properties of hydrocarbon fluids [47,93–96]. Complex physical and chemical reactions occur when different complex hydrocarbon compounds flow in micro- to nanopore throat media with different mineral properties [8,97]. In addition to the scale effect, this also includes the adsorption of crude oil components (e.g., gaseous hydrocarbons, saturated hydrocarbons, aromatic hydrocarbons, and asphaltenes) on different minerals [98–100]. Generally, adsorbed oil occurs in the form of high-density solidlike or embedded kerogen on the surface of minerals, and it is immovable without additional forces [47]. Considering the properties of oil in shale reservoirs, more light components are beneficial to an increase in movable oil contents [101,102].

On the other hand, reservoir conditions also play specific roles in controlling the flowability of shale oil, and fluid mobility is treated as weaker in small-scale pores (Figure 6) [71,103,104]. For example, the work of Zou et al. [49] found that the lower

threshold for oil storage and flow is a pore throat of 20 nm through simulations of a nanoporous template with a controllable pore diameter. At the same time, similar critical pore sizes, e.g., 10 nm [58,90,105], 12.1 nm [96], 30 nm [53], and 40 nm [106], for shale oil flows have been widely reported in related studies based on the SEM observations and quantitative calculation. A molecular dynamics simulation conducted by Wang et al. [107], through adsorption simulations of alkanes onto a graphene surface (oil-wet), proposed that alkanes only flowed after exceeding the critical pore size. The proportion of movable oil gradually increases with increasing pore size. Moreover, this work further realized that the fluidity of oil molecules in slit pores is better than that in circular pores (Figure 6). On the other hand, Cui and Cheng [108] suggested that movable shale oil was also related to the porosity, and the movable oil content increased with increasing porosity [60,89]. As mentioned above, the development of laminae can effectively improve the pore diameter, pore volume, and porosity of shale reservoir (Figures 3 and 4). Compared to massive shales, the laminated shales, thus, possess a higher movable oil proportion (Figure 7). Moreover, Ning et al. [58] and Jiang et al. [71] noted that the development of laminae can also increase the connectivity of the shale reservoir, which is conducive to improving the flow capacity of shale oil.

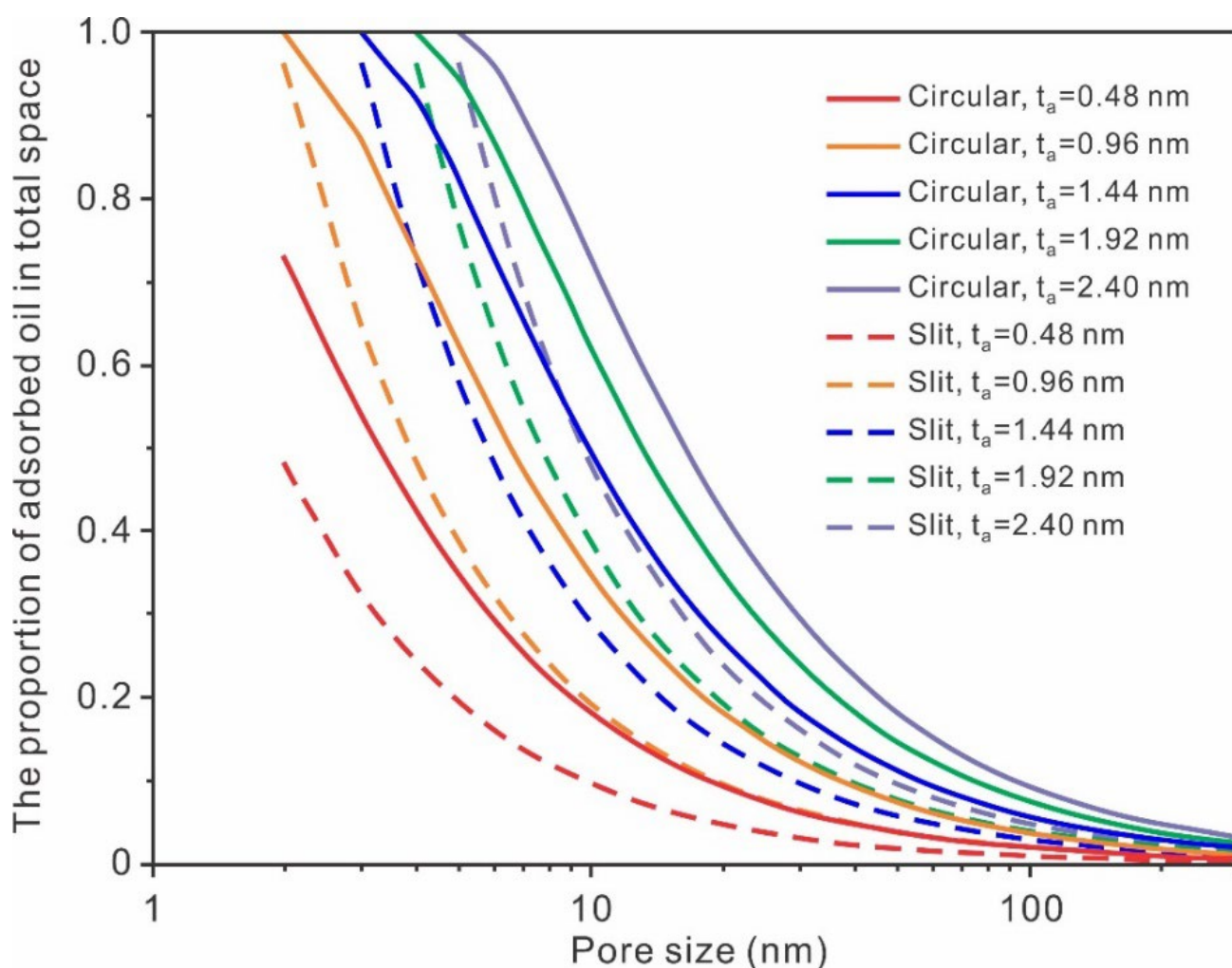


Figure 6. Effects of pore size, pore type, and adsorption layer thickness (t_a) on the proportion of adsorbed pore volume in the total space, modified after Wang et al. [107].

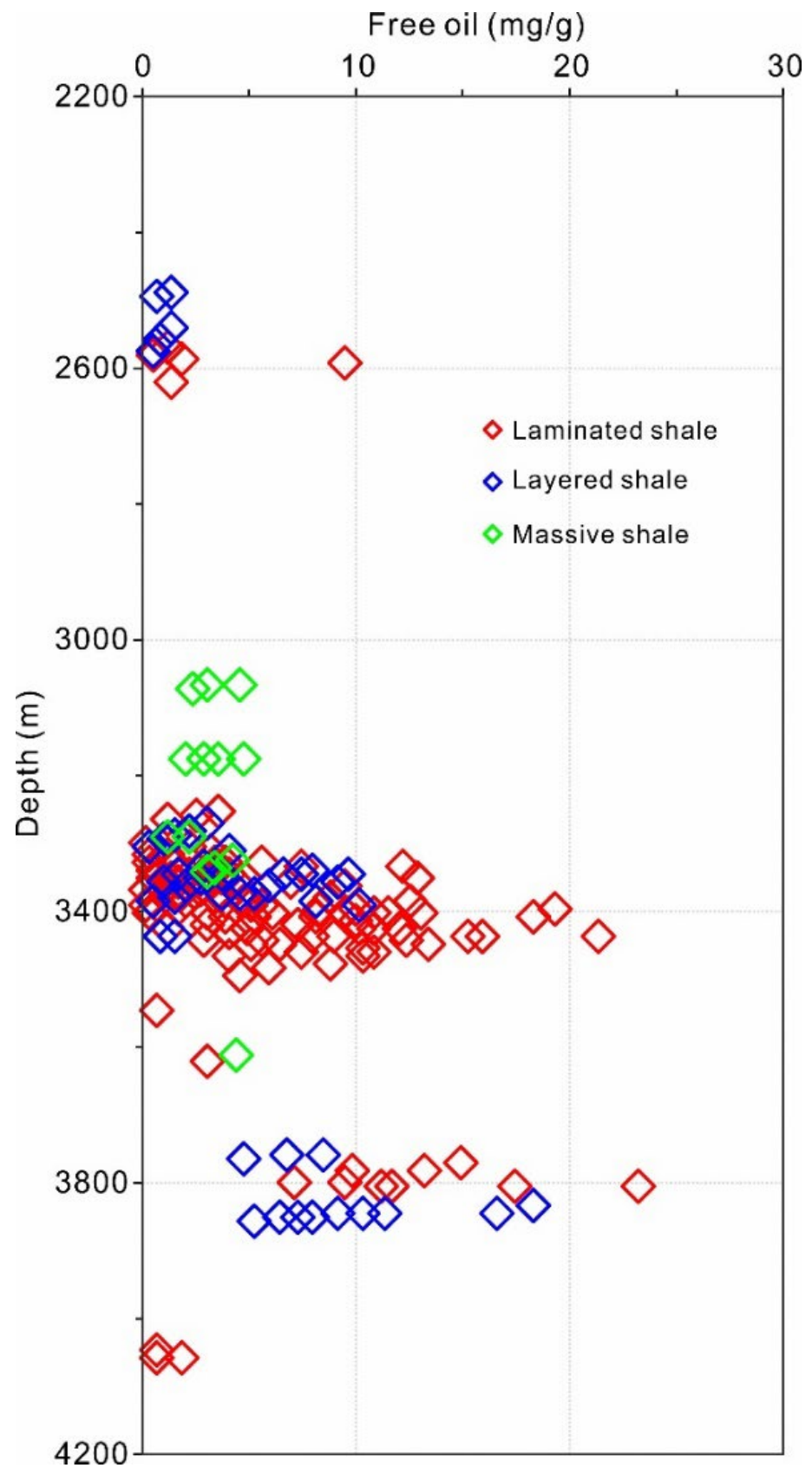


Figure 7. Difference in free oil in shale with different lamina structures, modified after Sun [59].

4.4. Impact of Laminae on Shale Fracability

Compared to conventional reservoirs, the physical characteristics and flow capacity of shale oil reservoirs are quite poor [109,110]. Therefore, using fracturing techniques is essential to connecting matrix pores and achieving commercial productivity of shale oil [111,112]. For this reason, fracability is an important factor to take into account when evaluating shale oil reservoirs [56,113,114]. Studies have demonstrated that shale texture clearly controls the compressive strengths, elastic moduli, and tensile strengths of fine-grained sedimentary rocks [56,109,110,114–117]. As for the fine-grained sedimentary rocks, laminated shale is often formed by alternating brittle laminae (e.g., carbonate lamina and felsic lamina) and plastic laminae (e.g., clay lamina and organic matter lamina) [11,16,21,22,97]. This situation enhanced the heterogeneity of the rock's physical properties and tended to concentrate stress [110]. In terms of the impact of structural weak surfaces, interfaces of brittle laminae and plastic laminae are essentially naturally occurring weak planes and frequently the focus of crack propagation [58,69]. An increase in their quantity facilitated the cracking of crack propagation along bedding surfaces [109,115,116], and complex networks of cracks are difficult to form in the process of fracturing (Figure 8A,B) [56,114,118]. Due to their great plasticity in particular, fractures that result from the fracturing of plastic laminae or structurally weak surface can be quickly repaired [56,110,114]. Wang et al. [119] conducted triaxial fracturing modeling experiments and found that lamination limits the height of hydraulic fracturing.

The influence of laminar thickness and laminar continuity on shale fracability was also investigated (Figure 8C–F). Some scholars found that, with the increase in laminar thickness, the weakening degree of laminae to rock decreases, and the brittle index of shale increases [114,118]. Accordingly, a negative correlation between the laminar thickness and shale fracability index (The fracability index is characterized as the ratio of the brittleness index to the fracture toughness. Generally, a higher fracturability index indicates a greater likelihood of the rock fracturing) was recognized (Figure 8C). Meanwhile, a positive correlation with Poisson's ratio was observed (Figure 8D). Notably, it does not seem that thicker laminae lead to a better fracturing effect. For example, Xu et al. [120] proposed that, when the thickness of shale laminae is moderate (~4 cm), more branching fractures could be recognized, and the fracturing result would be better. As for the laminar continuity, its influence on the fracability of shale is similar to the number of laminae (Figure 8E,F). Actually, this phenomenon is acceptable, as, when the continuity of laminae is great, the fracturing crack could mainly extend along the interface between different lamina, which would hinder the vertical bifurcation and turning of cracks [56,114,116,118].

To sum up, from the above discussion, shale fracturing is reduced with well-developed and strongly continued laminae, but enhanced with laminar thickness (Figure 8). However, it is worth clarifying that laminated shales have high porosity, large pore diameter, good pore connectivity, superior oil content, and great mobility [8,9,13,58,59]. More importantly, interfaces of brittle and plastic laminae are usually the main storage space for shale oil [75,83,84]. The above two factors make it possible to obtain high production even if only simple fractures are formed during fracturing in laminated shales [58,59]. Therefore, laminated shales, e.g., laminated argillaceous shales in the Jiyang Depression and laminated felsic shales in the Huanghua Depression, are usually characterized as the most favorable lithofacies among the continental shales in China [9,58,59,81,121].

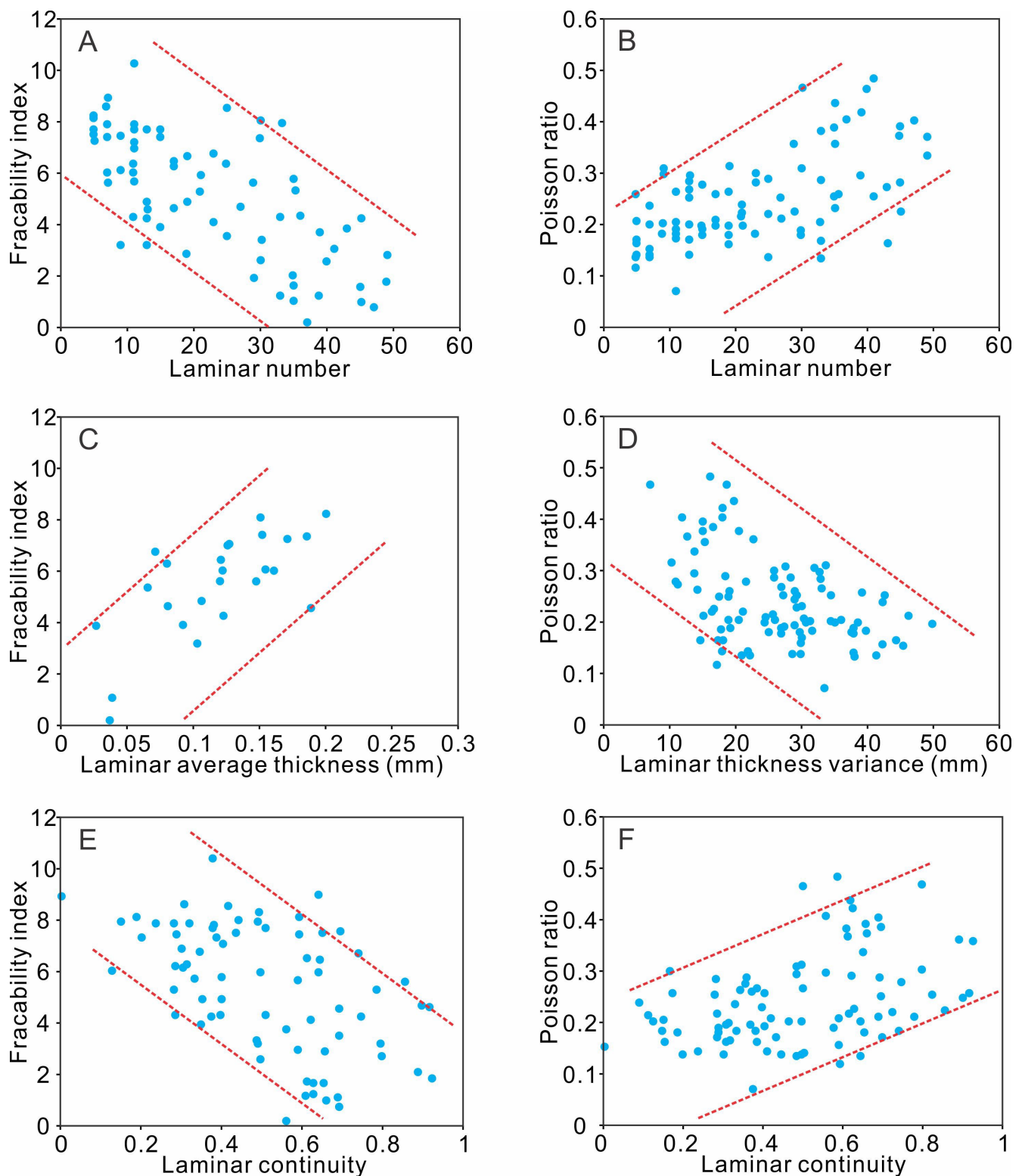


Figure 8. The influence of lamina structure on shale fracability, modified after Xiong et al. [56,114]. (A,B) The effects of lamina number on shale fracability index and Poisson's ratio. (C,D) The effects of lamina average thickness on shale fracability index and Poisson's ratio. (E,F) The effects of lamina continuity on shale fracability index and Poisson's ratio.

5. Conclusions

- (1) Sedimentary lamination is the most important visible sedimentary structure in fine-grained shales. The scales and types of laminae are also multiple. The multiscale laminar structure ranges from macroscopic lithology changes to microcosmic mineral superimposition and can be identified from shale systems. The combination of various probe techniques provides a method for the fine evaluation of multiscale laminae.
- (2) The development of laminae facilitates the formation of microfractures in the shale along the laminar direction. In particular, laminated shales have been identified as generally possessing a greater TOC content and, therefore, superior hydrocarbon generation capacity. These two factors allow the laminated shale to retain and store considerable petroleum even with a higher hydrocarbon expulsion efficiency. In addition, the large pore diameter and good pore connectivity increase the proportion of movable oil. Collectively, the laminated texture controls the shale oil enrichment characteristics.
- (3) The laminar structure also plays an important role in controlling shale fracability. Specifically, fracability declines with increasing laminar number and continuity, but increases with the improvement of laminar thickness. Notably, the high oil content and mobility in the laminated shale allow for high production even if only simple fractures are formed during the fracturing process.
- (4) The laminar structure impacts scale exploration and efficient development of oil. Thus, it is important to strengthen the research on the genetic mechanism and development distribution of laminar for the prediction of shale oil sweet spots. Furthermore, the recognition methods of seismic and logging for the identification and prediction of shale laminae should receive more attention in future work.

Author Contributions: S.X.: conceptualization, validation, resources, data curation, writing—review and editing, supervision, project administration, funding acquisition; Q.G.: methodology, software, formal analysis, investigation, resources, writing—original draft preparation, visualization. All authors have read and agreed to the published version of the manuscript.

Funding: This research was supported by the Shandong Provincial Key Research and Development Program (2020ZLYS08), the National Natural Science Foundation of China (42122017 and 41821002), the independent innovation research program of China University of Petroleum (East China) (21CX06001A), the Open Fund of Key Laboratory of Tectonics and Petroleum Resources (China University of Geosciences), Ministry of Education, China (TPR-2022-19), and the Fundamental Research Funds for National Universities, China University of Geosciences (Wuhan).

Data Availability Statement: The data presented in this study is available on request from the corresponding author.

Conflicts of Interest: The authors declare that they have no conflict of interest.

References

1. Katz, B.; Lin, F. Lacustrine basin unconventional resource plays: Key differences. *Mar. Pet. Geol.* **2014**, *56*, 255–265. [[CrossRef](#)]
2. Li, H. Research progress on evaluation methods and factors influencing shale brittleness: A review. *Energy Rep.* **2022**, *8*, 4344–4358. [[CrossRef](#)]
3. Li, H.; Zhou, J.; Mou, X.; Guo, H.; Wang, X.; An, H.; Mo, Q.; Long, H.; Dang, C.; Wu, J.; et al. Pore structure and fractal characteristics of the marine shale of the Longmaxi Formation in the Changning Area, Southern Sichuan Basin, China. *Front. Earth Sci.* **2022**, *10*, 1018274. [[CrossRef](#)]
4. Fan, C.; Li, H.; Qin, Q.; He, S.; Zhong, C. Geological conditions and exploration potential of shale gas reservoir in Wufeng and Longmaxi Formation of southeastern Sichuan Basin, China. *J. Pet. Sci. Eng.* **2020**, *191*, 107138. [[CrossRef](#)]
5. Li, J.; Li, H.; Yang, C.; Wu, Y.; Gao, Z.; Jiang, S. Geological characteristics and controlling factors of deep shale gas enrichment of the Wufeng-Longmaxi Formation in the southern Sichuan Basin, China. *Lithosphere* **2022**, *12*, 4737801. [[CrossRef](#)]
6. Gou, Q.; Xu, S.; Hao, F.; Lu, Y.; Shu, Z.; Lu, Y.; Wang, Z.; Wang, Y. Evaluation of the exploration prospect and risk of marine gas shale, southern China: A case study of Wufeng-Longmaxi shales in the Jiaoshiba area and Niutitang shales in the Cen'gong area. *GSA Bull.* **2022**, *134*, 1585–1602. [[CrossRef](#)]

7. Zou, C.; Pan, S.; Horsfield, B.; Yang, Z.; Hao, S.; Liu, E.; Zhang, L. Oil retention and intrasource migration in the organic-rich lacustrine Chang 7 shale of the Upper Triassic Yanchang Formation, Ordos Basin, central China. *AAPG Bull.* **2019**, *103*, 2627–2663. [[CrossRef](#)]
8. Jin, Z.; Zhu, R.; Liang, X.; Shen, Y. Several issues worthy of attention in current lacustrine shale oil exploration and development. *Pet. Explor. Dev.* **2021**, *48*, 1471–1484. [[CrossRef](#)]
9. Jin, Z.; Wang, G.; Liu, G.; Gao, B.; Liu, Q.; Wang, H.; Liang, X.; Wang, R. Research progress and key scientific issues of continental shale oil in China. *Acta Pet. Sin.* **2021**, *42*, 821–835. (In Chinese with English abstract)
10. Wang, X.; Zhang, G.; Tang, W.; Wang, D.; Wang, K.; Liu, J.; Du, D. A review of commercial development of continental shale oil in China. *Energy Geosci.* **2022**, *3*, 282–289. [[CrossRef](#)]
11. Wu, S.; Zhu, R.; Luo, Z.; Yang, Z.; Jiang, X.; Lin, M.; Su, L. Laminar structure of typical continental shales and reservoir quality evaluation in central-western basins in China. *China Pet. Explor.* **2022**, *27*, 62–72. (In Chinese with English abstract)
12. Li, Y.; Zhao, Q.; Lyu, Q.; Xue, Z.; Cao, X.; Liu, Z. Evaluation technology and practice of continental shale oil development in China. *Pet. Explor. Dev.* **2022**, *49*, 1098–1109. [[CrossRef](#)]
13. Zhao, W.; Zhu, R.; Liu, W.; Bian, C.; Wang, K. Enrichment conditions and occurrence features of lacustrine mid-high matured shale oil in onshore China. *Earth Sci. Front.* **2023**, *30*, 116–127. (In Chinese with English abstract) [[CrossRef](#)]
14. Bohacs, K.M.; Carroll, A.R.; Neal, J.E.; Mankiewicz, P.J. Lake-basin type, source potential, and hydrocarbon character: An integrated sequence-stratigraphic-geochemical framework. In *Lake Basins through Space and Time*; American Association of Petroleum Geologists: Tulsa, OK, USA, 2000; pp. 3–34.
15. Shi, J.; Jin, Z.; Liu, Q.; Fan, T.; Gao, Z. Sunspot cycles recorded in Eocene lacustrine fine-grained sedimentary rocks in the Bohai Bay Basin, eastern China. *Glob. Planet. Change* **2021**, *205*, 103614. [[CrossRef](#)]
16. Liang, C.; Cao, Y.; Jiang, Z.; Wu, J.; Song, G.; Wang, Y. Shale oil potential of lacustrine black shale in the Eocene Dongying depression: Implications for geochemistry and reservoir characteristics. *AAPG Bull.* **2017**, *101*, 1835–1858. [[CrossRef](#)]
17. Li, L.; Huang, B.; Li, Y.; Hu, R.; Li, X. Multi-scale modeling of shale laminas and fracture networks in the Yanchang formation, Southern Ordos Basin, China. *Eng. Geol.* **2018**, *243*, 231–240. [[CrossRef](#)]
18. Wang, M.; Guan, Y.; Li, C.; Liu, Y.; Liu, W. Qualitative description and full-pore-size quantitative evaluation of pores in lacustrine shale reservoir of Shahejie Formation, Jiyang Depression. *Oil Gas Geol.* **2018**, *39*, 1107–1119.
19. Zhang, L.; Chen, Z.; Li, Z.; Zhang, S.; Li, J.; Liu, Q.; Zhu, R.; Zhang, J.; Bao, Y. Structural features and genesis of microscopic pores in lacustrine shale in an oil window: A case study of the Dongying depression. *AAPG Bull.* **2019**, *103*, 1889–1924. [[CrossRef](#)]
20. Xu, Q.; Zhao, X.; Pu, X.; Han, W.; Shi, Z.; Tian, J.; Zhang, B.; Xin, B.; Guo, P. Characteristics and Control Mechanism of Lacustrine Shale Oil Reservoir in the Member 2 of Kongdian Formation in Cangdong Sag, Bohai Bay Basin, China. *Front. Earth Sci.* **2021**, *9*, 783042. [[CrossRef](#)]
21. Xin, B.; Zhao, X.; Hao, F.; Jin, F.; Pu, X.; Han, W.; Xu, Q.; Guo, P.; Tian, J. Laminae characteristics of lacustrine shales from the Paleogene Kongdian Formation in the Cangdong Sag, Bohai Bay Basin, China: Why do laminated shales have better reservoir physical properties? *Int. J. Coal Geol.* **2022**, *260*, 104056. [[CrossRef](#)]
22. Shi, J.; Jin, Z.; Liu, Q.; Zhang, T.; Fan, T.; Gao, Z. Laminar characteristics of lacustrine organic-rich shales and their significance for shale reservoir formation: A case study of the Paleogene shales in the Dongying Sag, Bohai Bay Basin, China. *J. Asian Earth Sci.* **2022**, *223*, 104976. [[CrossRef](#)]
23. Zhao, X.; Zhou, L.; Pu, X.; Jin, F.; Han, W.; Xiao, D.; Chen, S.; Shi, Z.; Zhang, W.; Yang, F. Geological characteristics of shale rock system and shale oil exploration breakthrough in a lacustrine basin: A case study from the Paleogene 1st sub-member of Kong 2 Member in Cangdong Sag, Bohai Bay Basin, China. *Pet. Explor. Dev.* **2018**, *45*, 377–388. [[CrossRef](#)]
24. Li, M.; Wu, S.; Hu, S.; Zhu, R.; Meng, S.; Yang, J. Lamination Texture and Its Effects on Reservoir and Geochemical Properties of the Palaeogene Kongdian Formation in the Cangdong Sag, Bohai Bay Basin, China. *Minerals* **2021**, *11*, 1360. [[CrossRef](#)]
25. Pang, X.J.; Wang, G.W.; Kuang, L.C.; Lai, J.; Gao, Y.; Zhao, Y.; Li, H.; Wang, S.; Bao, M.; Liu, S.; et al. Prediction of multiscale laminae structure and reservoir quality in fine-grained sedimentary rocks: The Permian Lucaogou Formation in Jimusar Sag, Junggar Basin. *Pet. Sci.* **2022**, *19*, 2549–2571. [[CrossRef](#)]
26. Ingram, R.L. Terminology for the thickness of stratification and parting units in sedimentary rocks. *GSA Bull.* **1954**, *65*, 937–938. [[CrossRef](#)]
27. Liu, H.; Wang, Y.; Yang, Y.; Zhang, S. Sedimentary environment and lithofacies of fine-grained hybrid in Dongying Sag: A case of fine-grained sedimentary system of the Es4. *Earth Sci.* **2020**, *45*, 3543–3555.
28. Anderson, R.Y. Seasonal sedimentation: A framework for reconstructing climatic and environmental change. Geological Society, London. *Spec. Publ.* **1996**, *116*, 1–15. [[CrossRef](#)]
29. Chen, S.; Zhang, S.; Liu, H.; Yan, J. Discussion on mixing of fine-grained sediments in lacustrine deep water. *J. Palaeogeogr.* **2017**, *19*, 271–284.
30. Wang, S.; Wang, G.; Huang, L.; Song, L.; Zhang, Y.; Li, D.; Huang, Y. Logging evaluation of lamina structure and reservoir quality in shale oil reservoir of Fengcheng Formation in Mahu Sag, China. *Mar. Pet. Geol.* **2021**, *133*, 105299. [[CrossRef](#)]
31. Rickman, R.; Mullen, M.J.; Petre, J.E.; Grieser, B.; Kundert, D. A practical use of shale petrophysics for stimulation design optimization: All shale plays are not clones of the Barnett Shale. In Proceedings of the SPE Annual Technical Conference and Exhibition, Denver, CO, USA, 21–24 September 2008; p. SPE-115258-MS. [[CrossRef](#)]

32. Aplin, A.C.; Macquaker, J.H.S. Mudstone diversity: Origin and implications for source, seal, and reservoir properties in petroleum systems. *AAPG Bull.* **2011**, *95*, 2031–2059. [[CrossRef](#)]
33. Ji, W.; Song, Y.; Jiang, Z.; Chen, L.; Li, Z.; Yang, X.; Meng, M. Estimation of marine shale methane adsorption capacity based on experimental investigations of Lower Silurian Longmaxi formation in the Upper Yangtze Platform, south China. *Mar. Pet. Geol.* **2015**, *68*, 94–106. [[CrossRef](#)]
34. Lai, J.; Wang, G.; Fan, Z.; Chen, J.; Wang, S.; Fan, X. Sedimentary characterization of a braided delta using well logs: The Upper Triassic Xujiahe formation in central Sichuan basin, China. *J. Pet. Sci. Eng.* **2017**, *154*, 172–193. [[CrossRef](#)]
35. Campbell, C.V. Lamina, laminaset, bed and bedset. *Sedimentology* **1967**, *8*, 7–26. [[CrossRef](#)]
36. Jiang, Z.; Chen, D.; Qiu, L.; Liang, H.; Ma, J. Source-controlled carbonates in a small Eocene half-graben lake basin (Shulu Sag) in central Hebei Province, North China. *Sedimentology* **2007**, *54*, 265–292. [[CrossRef](#)]
37. Lazar, O.R.; Bohacs, K.M.; Macquaker, J.H.S.; Schieber, J.; Demko, T.M. Capturing key attributes of fine-grained sedimentary rocks in outcrops, cores, and thin sections: Nomenclature and description guidelines. *J. Sediment. Res.* **2015**, *85*, 230–246. [[CrossRef](#)]
38. Liu, G.; Huang, Z.; Jiang, Z.; Chen, J.; Chen, C.; Gao, X. The characteristic and reservoir significance of lamina in shale from Yanchang Formation of Ordos Basin. *Nat. Gas Geosci.* **2015**, *26*, 408–411. (In Chinese with English abstract)
39. Shi, Z.; Qiu, Z. Main bedding types of marine fine-grained sediments and their significance for oil and gas exploration and development. *Acta Sedimentol. Sin.* **2021**, *39*, 181–196. (In Chinese with English abstract)
40. Liang, C.; Wu, J.; Cao, Y.; Liu, K.; Khan, D. Storage space development and hydrocarbon occurrence model controlled by lithofacies in the Eocene Jiyang Sub-basin, East China: Significance for shale oil reservoir formation. *J. Pet. Sci. Eng.* **2022**, *2015*, 110631. [[CrossRef](#)]
41. Dong, C.; Ma, C.; Lin, C.; Sun, X.; Yuan, M. A method of classification of shale set. *J. China Univ. Pet.* **2015**, *39*, 1–7. (In Chinese with English abstract)
42. Hua, G.L.; Wu, S.T.; Qiu, Z.; Jing, Z.; Xu, J.; Guan, M. Lamination texture and its effect on reservoir properties: A case study of Longmaxi Shale, Sichuan Basin. *Acta Sedimentol. Sin.* **2021**, *32*, 1–22.
43. Xing, M.; Chen, L.; Chen, X.; Ji, Y.; Wu, P.; Hu, Y.; Wang, G.; Peng, H. Characteristics, genetic mechanism of marine shale laminae and its significance of shale gas accumulation. *J. Cent. South Univ. (Sci. Technol.)* **2022**, *53*, 3490–3508. (In Chinese with English abstract)
44. Jarvie, D.M. Shale resource systems for oil and gas: Part 2—Shale-oil resource systems. In *Shale Reservoirs—Giant Resources for the 21st Century: AAPG Memoir 97*; American Association of Petroleum Geologists: Tulsa, OK, USA, 2012; pp. 89–119.
45. Liu, X.; Zhang, D. A review of phase behavior simulation of hydrocarbons in confined space: Implications for shale oil and shale gas. *J. Nat. Gas Sci. Eng.* **2019**, *68*, 102901. [[CrossRef](#)]
46. Zhu, C.; Guo, W.; Li, Y.; Gong, H.; Sheng, J.; Dong, M. Effect of occurrence states of fluid and pore structures on shale oil movability. *Fuel* **2021**, *288*, 119847. [[CrossRef](#)]
47. Feng, Y.; Xiao, X.; Wang, E.; Sun, J.; Gao, P. Oil retention in shales: A review of the mechanism, controls and assessment. *Front. Earth Sci.* **2021**, *9*, 720839. [[CrossRef](#)]
48. Chen, G.; Lu, S.; Zhang, J.; Pervukhina, M.; Liu, K.; Wang, M.; Han, T.; Tian, S.; Li, J.; Zhang, Y.; et al. A method for determining oil-bearing pore size distribution in shales: A case study from the Damintun Sag, China. *J. Pet. Sci. Eng.* **2018**, *166*, 673–678. [[CrossRef](#)]
49. Zou, C.; Jin, X.; Zhu, R.; Gong, G.; Sun, L.; Dai, J.; Meng, D.; Wang, X.; Li, J.; Wu, S.; et al. Do shale pore throats have a threshold diameter for oil storage? *Sci. Rep.* **2015**, *5*, 1–6. [[CrossRef](#)]
50. Wu, S.T.; Zou, C.N.; Zhu, R.K.; Yuan, X.; Yao, J.; Yang, Z.; Liang, S.; Bai, B. Reservoir quality characterization of upper triassic Chang 7 shale in Ordos basin. *Earth Sci.* **2015**, *40*, 1810–1823.
51. Johnson, R.C.; Birdwell, J.E.; Mercier, T.J.; Brownfield, M.E. Geology of tight oil and potential tight oil reservoirs in the lower part of the Green River Formation, Uinta, Piceance, and Greater Green River Basins, Utah, Colorado, and Wyoming. *US Geol. Surv.* **2016**. [[CrossRef](#)]
52. Schimmelmann, A.; Lange, C.B.; Schieber, J.; Francus, P.; Ojala, A.E.K.; Zolitschka, B. Varves in marine sediments: A review. *Earth-Sci. Rev.* **2016**, *159*, 215–246. [[CrossRef](#)]
53. Wang, M.; Ma, R.; Li, J.; Lu, S.; Li, C.; Guo, Z.; Li, Z. Occurrence mechanism of lacustrine shale oil in the Paleogene Shahejie Formation of Jiyang depression, Bohai Bay Basin, China. *Pet. Explor. Dev.* **2019**, *46*, 833–846. [[CrossRef](#)]
54. Ma, C.; Elsworth, D.; Dong, C.; Lin, C.; Luan, G.; Chen, B.; Liu, X.; Muhammad, J.M.; Muhammad, A.Z.; Shen, Z.; et al. Controls of hydrocarbon generation on the development of expulsion fractures in organic-rich shale: Based on the Paleogene Shahejie Formation in the Jiyang Depression, Bohai Bay Basin, East China. *Mar. Pet. Geol.* **2017**, *86*, 1406–1416. [[CrossRef](#)]
55. Li, H.; Tang, H.; Qin, Q.; Zhou, J.; Qin, Z.; Fan, C.; Su, P.; Wang, Q.; Zhong, C. Characteristics, formation periods and genetic mechanisms of tectonic fractures in the tight gas sandstones reservoir: A case study of Xujiahe Formation in YB area, Sichuan Basin, China. *J. Pet. Sci. Eng.* **2019**, *178*, 723–735. [[CrossRef](#)]
56. Xiong, Z.; Wang, G.; Cao, Y.; Liang, C.; Li, M.; Shi, X.; Zhang, B.; Li, J.; Fu, Y. Controlling effect of texture on fracability in lacustrine fine-grained sedimentary rocks. *Mar. Pet. Geol.* **2019**, *101*, 195–210. [[CrossRef](#)]
57. Wang, Y.; Wang, X.; Song, G.; Liu, H.; Zhu, D.; Zhu, D.; Ding, J.; Yang, W.; Yin, Y.; Zhang, S.; et al. Genetic connection between mud shale lithofacies and shale oil enrichment in Jiyang Depression, Bohai Bay Basin. *Pet. Explor. Dev.* **2016**, *43*, 759–768. [[CrossRef](#)]

58. Ning, F.; Wang, X.; Hao, X.; Yang, W.; Yin, Y.; Ding, J.; Zhu, D.; Zhu, D.; Zhu, J. Occurrence mechanism of shale oil with different lithofacies in Jiyang Depression. *Acta Pet. Sin.* **2017**, *38*, 185–195.
59. Sun, H.Q. Exploration practice and cognitions of shale oil in Jiyang depression. *China Pet. Explor.* **2017**, *22*, 1–14.
60. Bao, Y.S. Effective reservoir spaces of Paleogene shale oil in the Dongying Depression, Bohai Bay Basin. *Pet. Geol. Experiment* **2018**, *40*, 480–484. (In Chinese with English abstract)
61. Zhang, L.; Bao, Y.S. Xi, C. Pore Structure Characteristics and Pore Connectivity of Paleogene Shales in Dongying Depression. *Xinjiang Pet. Geol.* **2018**, *39*, 134–139. (In Chinese with English abstract)
62. Hu, Q.; Zhang, X.; Meng, X.; Li, Z.; Xie, Z.; Li, M. Characterization of micro-nano pore networks in shale oil reservoirs of Paleogene Shahejie Formation in Dongying Sag of Bohai Bay Basin, East China. *Pet. Explor. Dev.* **2017**, *44*, 720–730. [[CrossRef](#)]
63. Hu, Q.; Liu, H.; Li, M.; Li, Z.; Yang, R.; Zhang, Y.; Sun, M. Wettability, pore connectivity and fluid-tracer migration in shale oil reservoirs of Paleogene Shahejie Formation in Dongying sag of Bohai Bay Basin, East China. *Acta Pet. Sin.* **2018**, *39*, 278–289.
64. Teng, J.; Liu, H.; Qiu, L.; Zhang, S.; Hao, Y.; Tian, F.; Zhu, L.; Fang, Z. Control law of material components of shale oil reservoir on oil-bearing characteristics in Jiyang Depression. *Editor. Dep. Pet. Geol. Recovery Effic.* **2019**, *26*, 80–87. (In Chinese with English abstract)
65. Song, M.S. Practice and current status of shale oil exploration in Jiyang Depression. *Editorial Dep. Pet. Geol. Recovery Effic.* **2019**, *26*, 1–12. (In Chinese with English abstract)
66. Li, T.; Jiang, Z.; Su, P.; Zhang, X.; Chen, W.; Wang, X.; Ning, C.; Wang, Z.; Xue, Z. Effect of laminae development on pore structure in the lower third member of the Shahejie Shale, Zhanhua Sag, Eastern China. *Interpretation* **2020**, *8*, T103–T114. [[CrossRef](#)]
67. Chen, S.; Zhang, S.; Wang, Y.; Tan, M. Lithofacies types and reservoirs of Paleogene fine-grained sedimentary rocks Dongying Sag, Bohai Bay Basin, China. *Pet. Explor. Dev.* **2016**, *43*, 218–229. [[CrossRef](#)]
68. Liu, H.M.; Zhang, S.; Bao, S.Y.; Fang, Z.; Yao, S.; Wang, Y. Geological characteristics and effectiveness of the shale oil reservoir in Dongying sag. *Oil Gas Geol.* **2019**, *40*, 512–523.
69. Song, M.; Liu, H.; Wang, Y.; Liu, Y. Enrichment rules and exploration practices of Paleogene shale oil in Jiyang Depression, Bohai Bay Basin, China. *Pet. Explor. Dev.* **2020**, *47*, 225–235. [[CrossRef](#)]
70. Hu, S.; Zhao, W.; Hou, L.; Yan, Z.; Zhu, R.; Wu, S.; Bai, B.; Jin, X. Development potential and technical strategy of continental shale oil in China. *Pet. Explor. Dev.* **2020**, *47*, 877–887. [[CrossRef](#)]
71. Jiang, Z.; Li, T.; Gong, H.; Jiang, T.; Chang, J.; Ning, C.; Su, S.; Chen, W. Characteristics of low-mature shale reservoirs in Zhanhua Sag and their influence on the mobility of shale oil. *Acta Pet. Sin.* **2020**, *41*, 1587–1600.
72. Zhang, S. Shale oil enrichment elements and geological desert types in Jiyang Depression. *Sci. Technol. Eng.* **2021**, *21*, 504–511. (In Chinese with English abstract)
73. Gou, Q.; Xu, S.; Hao, F.; Yang, F.; Zhang, B.; Shu, Z.; Zhang, A.; Wang, Y.; Cheng, X.; Qing, J.; et al. Full-scale pores and micro-fractures characterization using FE-SEM, gas adsorption, nano-CT and micro-CT: A case study of the Silurian Longmaxi Formation shale in the Fuling area, Sichuan Basin, China. *Fuel* **2019**, *253*, 167–179. [[CrossRef](#)]
74. Gou, Q.; Xu, S.; Hao, F.; Yang, F.; Shu, Z.; Liu, R. The effect of tectonic deformation and preservation condition on the shale pore structure using adsorption-based textural quantification and 3D image observation. *Energy* **2021**, *219*, 119579. [[CrossRef](#)]
75. Guan, M.; Liu, X.; Jin, Z.; Lai, J.; Liu, J.; Sun, B.; Liu, T.; Hua, Z.; Xu, W.; Shu, H.; et al. Quantitative characterization of various oil contents and spatial distribution in lacustrine shales: Insight from petroleum compositional characteristics derived from programmed pyrolysis. *Mar. Pet. Geol.* **2022**, *138*, 105522. [[CrossRef](#)]
76. Liu, X.; Lai, J.; Fan, X.; Shu, H.; Wang, G.; Ma, X.; Liu, M.; Guan, M.; Luo, Y. Insights in the pore structure, fluid mobility and oiliness in oil shales of Paleogene Funing Formation in Subei Basin, China. *Mar. Pet. Geol.* **2020**, *114*, 104228. [[CrossRef](#)]
77. Xu, Y.; Lun, Z.M.; Pan, Z.J.; Wang, H.; Zhou, X.; Zhao, C.; Zhang, D. Occurrence space and state of shale oil: A review. *J. Pet. Sci. Eng.* **2022**, *211*, 110183. [[CrossRef](#)]
78. Li, Z.; Qian, M.; Li, M.; Jiang, Q.; Liu, P.; Rui, X.; Cao, T.; Pan, Y. Oil content and occurrence in low-medium mature organic-rich lacustrine shales: A case from the 1st member of the Eocene-Oligocene Shahejie Formation in Well Luo-63 and Yi-21, Bonan Subsag, Bohai Bay Basin. *Oil Gas Geol.* **2017**, *38*, 448–456.
79. Zeng, X.; Cai, J.; Dong, Z.; Wang, X.; Hao, Y. Sedimentary characteristics and hydrocarbon generation potential of mudstone and shale: A case study of Middle Submember of Member 3 and Upper Submember of Member 4 in Shahejie Formation in Dongying sag. *Acta Pet. Sin.* **2017**, *38*, 31–43.
80. Nikolaev, M.Y.; Kazak, A.V. Liquid saturation evaluation in organic-rich unconventional reservoirs: A comprehensive review. *Earth Sci. Rev.* **2019**, *194*, 327–349. [[CrossRef](#)]
81. Zhao, X.; Pu, X.; Zhou, L.; Jin, F.; Han, G.; Shi, Z.; Han, W.; Ding, Y.; Zhang, W.; Wang, G.; et al. Enrichment theory, exploration technology and prospects of shale oil in lacustrine facies zone of deep basin: A case study of the Paleogene in Huanghua Depression, Bohai Bay Basin. *Acta Pet. Sin.* **2021**, *42*, 143–162.
82. Du, J.; Hu, S.; Pang, Z.; Lin, S.; Hou, L.; Zhu, R. The types, potentials and prospects of continental shale oil in China. *China Pet. Explor.* **2019**, *24*, 560–568.
83. Zhou, L.; Zhao, X.; Chai, G.; Jiang, W.; Pu, X.; Wang, X.; Han, W.; Guan, Q.; Feng, J.; Liu, X. Key exploration & development technologies and engineering practice of continental shale oil: A case study of Member 2 of Paleogene Kongdian Formation in Cangdong Sag, Bohai Bay Basin, East China. *Pet. Explor. Dev.* **2020**, *47*, 1138–1146.

84. Zhao, W.; Zhu, R.; Hu, S.; Hou, L.; Wu, S. Accumulation contribution differences between lacustrine organic-rich shales and mudstones and their significance in shale oil evaluation. *Pet. Explor. Dev.* **2020**, *47*, 1160–1171. [[CrossRef](#)]
85. Ma, L.; Cheng, K.; Liu, D.; Xiong, Y. Laminae algal distribution characteristics of lower Cretaceous and the relation to oil-gas of Jiuquan Basin. *Acta Sedimentol. Sin.* **2007**, *25*, 147–153. (In Chinese with English abstract)
86. Zhang, S.C.; Zhang, L.Y.; Zha, M. Research on simulation of hydrocarbon expulsion difference in lacustrine source rocks: A case study of Paleogene Es3 member in the Dongying Depression. *Pet. Geol. Recovery Effic.* **2009**, *16*, 32–35. (In Chinese with English abstract)
87. Jin, Q.; Zhang, H.J.; Cheng, F.Q.; Xu, J. Stimulations on generation, expulsion and retention of liquid hydrocarbons in source rocks deposited in lacustrine basin and their significance in petroleum geology. *J. China Univ. Pet. (Ed. Nat. Sci.)* **2019**, *43*, 44–52. (In Chinese with English abstract)
88. Xi, K.; Li, K.; Cao, Y.; Lin, M.; Niu, X.; Zhu, R.; Wei, X.; You, Y.; Liang, X.; Feng, S. Laminae combination and shale oil enrichment patterns of Chang 73 sub-member organic-rich shales in the Triassic Yanchang Formation, Ordos Basin, NW China. *Pet. Explor. Dev.* **2020**, *47*, 1342–1353. [[CrossRef](#)]
89. Han, W.; Zhao, X.; Jin, F.; Pu, X.; Chen, S.; Mou, L.; Zhang, W.; Shi, Z.; Wang, H. Sweet spots evaluation and exploration of lacustrine shale oil of the 2nd member of Paleogene Kongdian Formation in Cangdong sag, Dagang Oilfield, China. *Pet. Explor. Dev.* **2021**, *48*, 1–10. [[CrossRef](#)]
90. Li, M.; Chen, Z.; Ma, X.; Cao, T.; Qian, M.; Jiang, Q.; Tao, G.; Li, Z.; Song, G. Shale oil resource potential and oil mobility characteristics of the eocene-oligocene Shahejie Formation, Jiyang super-depression, Bohai Bay Basin of China. *Int. J. Coal Geol.* **2019**, *204*, 130–143. [[CrossRef](#)]
91. Zhang, P.; Lu, S.; Lin, Z.; Duan, H.; Chang, X.; Qiu, Y.; Fu, Q.; Zhi, Q.; Wang, J.; Huang, H. Key Oil Content Parameter Correction of Shale Oil Resources: A Case Study of the Paleogene Funing Formation, Subei Basin, China. *Energy Fuels* **2022**, *36*, 5316–5326. [[CrossRef](#)]
92. Wang, E.; Li, C.; Feng, Y.; Song, Y.; Guo, T.; Li, M.; Chen, Z. Novel method for determining the oil moveable threshold and an innovative model for evaluating the oil content in shales. *Energy* **2022**, *239*, 121848. [[CrossRef](#)]
93. Teklu, T.W.; Alharthy, N.; Kazemi, H.; Yin, X.; Graves, R.M. Phase behavior and minimum miscibility pressure in nanopores. *SPE Reserv. Eval. Eng.* **2014**, *17*, 396–403. [[CrossRef](#)]
94. Hu, T.; Pang, X.; Jiang, S.; Wang, Q.; Zheng, X.; Ding, X.; Zhao, Y.; Zhu, C.; Li, H. Oil content evaluation of lacustrine organic-rich shale with strong heterogeneity: A case study of the Middle Permian Lucaogou Formation in Jimusaer Sag, Junggar Basin, NW China. *Fuel* **2018**, *221*, 196–205. [[CrossRef](#)]
95. Sobacki, N.; Nieto-Draghi, C.; Di Lella, A.; Ding, D.Y. Phase behavior of hydrocarbons in nano-pores. *Fluid Phase Equilibria* **2019**, *497*, 104–121. [[CrossRef](#)]
96. Zhu, X.; Cai, J.; Liu, Q.; Li, Z.; Zhang, X. Thresholds of petroleum content and pore diameter for petroleum mobility in shale. *AAPG Bull.* **2019**, *103*, 605–617. [[CrossRef](#)]
97. Liang, C.; Cao, Y.; Liu, K.; Jiang, Z.; Wu, J.; Hao, F. Diagenetic variation at the lamina scale in lacustrine organic-rich shales: Implications for hydrocarbon migration and accumulation. *Geochim. Cosmochim. Acta* **2018**, *229*, 112–128. [[CrossRef](#)]
98. Ribeiro, R.C.; Correia, J.C.G.; Seidl, P.R. The influence of different minerals on the mechanical resistance of asphalt mixtures. *J. Pet. Sci. Eng.* **2009**, *65*, 171–174. [[CrossRef](#)]
99. Mohammadi, M.; Sedighi, M. Modification of Langmuir isotherm for the adsorption of asphaltene or resin onto calcite mineral surface: Comparison of linear and non-linear methods. *Prot. Met. Phys. Chem. Surf.* **2013**, *49*, 460–470. [[CrossRef](#)]
100. Tian, S.; Erastova, V.; Lu, S.; Greenwell, H.C.; Underwood, T.R.; Xue, H.; Zeng, F.; Chen, G.; Wu, C.; Zhao, R. Understanding model crude oil component interactions on kaolinite silicate and aluminol surfaces: Toward improved understanding of shale oil recovery. *Energy Fuels* **2018**, *32*, 1155–1165. [[CrossRef](#)]
101. Jarvie, D.M. Components and processes affecting producibility and commerciality of shale resource systems. *Geol. Acta* **2014**, *12*, 307–325.
102. Fan, B.; Shi, L. Deep-lacustrine shale heterogeneity and its impact on hydrocarbon generation, expulsion, and retention: A case study from the upper triassic Yanchang Formation, Ordos Basin, China. *Nat. Resour. Res.* **2019**, *28*, 241–257. [[CrossRef](#)]
103. Dillinger, A.; Esteban, L. Experimental evaluation of reservoir quality in Mesozoic formations of the Perth Basin (Western Australia) by using a laboratory low field nuclear magnetic resonance. *Mar. Pet. Geol.* **2014**, *57*, 455–469. [[CrossRef](#)]
104. Ning, C.; Ma, Z.; Jiang, Z.; Su, S.; Li, T.; Zheng, L.; Wang, G.; Li, F. Effect of shale reservoir characteristics on shale oil movability in the lower third member of the Shahejie Formation, Zhanhua Sag. *Acta Geol. Sin. Engl. Ed.* **2020**, *94*, 352–363. [[CrossRef](#)]
105. Sun, C.; Yao, S.; Li, J.; Liu, B.; Liu, H.; Xie, Z. Characteristics of pore structure and effectiveness of shale oil reservoir space in Dongying Sag, Jiyang Depression, Bohai Bay Basin. *J. Nanosci. Nanotechnol.* **2017**, *17*, 6781–6790. [[CrossRef](#)]
106. Pan, Y.; Huang, Z.; Guo, X.; Liu, B.; Wang, G.; Xu, X. Study on the pore structure, fluid mobility, and oiliness of the lacustrine organic-rich shale affected by volcanic ash from the Permian Lucaogou Formation in the Santanghu Basin, Northwest China. *J. Pet. Sci. Eng.* **2022**, *208*, 109351. [[CrossRef](#)]
107. Wang, S.; Feng, Q.; Javadpour, F.; Xia, T.; Li, Z. Oil adsorption in shale nanopores and its effect on recoverable oil-in-place. *Int. J. Coal Geol.* **2015**, *147*, 9–24. [[CrossRef](#)]
108. Cui, J.; Cheng, L. A theoretical study of the occurrence state of shale oil based on the pore sizes of mixed Gaussian distribution. *Fuel* **2017**, *206*, 564–571. [[CrossRef](#)]

109. Tan, P.; Jin, Y.; Han, K.; Hou, B.; Chen, M.; Guo, X.; Gao, J. Analysis of hydraulic fracture initiation and vertical propagation behavior in laminated shale formation. *Fuel* **2017**, *206*, 482–493. [[CrossRef](#)]
110. Ma, C.; Dong, C.; Lin, C.; Elsworth, D.; Luan, G.; Sun, X.; Liu, X. Influencing factors and fracability of lacustrine shale oil reservoirs. *Mar. Pet. Geol.* **2019**, *110*, 463–471. [[CrossRef](#)]
111. Sheng, Q.; Li, W. Evaluation method of shale fracability and its application in Jiaoshiba area. *Prog. Geophys.* **2016**, *31*, 1473–1479.
112. Osipov, A.A. Fluid mechanics of hydraulic fracturing: A review. *J. Pet. Sci. Eng.* **2017**, *156*, 513–535. [[CrossRef](#)]
113. Chong, K.K.; Grieser, W.V.; Passman, A.; Tamayo, C.H.; Modeland, N.; Burke, B. A completions guide book to shale-play development: A review of successful approaches towards shale-play stimulation in the last two decades. In Proceedings of the Canadian Unconventional Resources and International Petroleum Conference, Calgary, AB, Canada, 19–21 October 2010; pp. SPE-133874-MS. [[CrossRef](#)]
114. Xiong, Z.; Cao, Y.; Wang, G.; Liang, C.; Shi, X.; Li, M.; Fu, Y.; Zhao, S. Influence of laminar structure differences on the fracability of lacustrine fine-grained sedimentary rocks. *Acta Pet. Sin.* **2019**, *40*, 74–85.
115. Zhao, W.; Hou, G.; Zhang, J.; Feng, S.; Ju, W.; You, Y.; Yu, X.; Zhan, Y. Study on the development law of structural fractures of Yanchang Formation in Longdong Area, Ordos Basin. *Acta Sci. Nat. Univ. Pekin.* **2015**, *51*, 1047–1058. (In Chinese with English abstract)
116. Heng, S.; Yang, C.; Guo, Y.; Wang, C.; Wang, L. Influence of bedding planes on hydraulic fracture propagation in shale formation. *J. Rock Mech. Eng.* **2015**, *34*, 228–237. (In Chinese with English abstract)
117. Gao, H.; Zhang, X.; He, M.; Xu, C.; Dou, L.; Zhu, G.; Li, Y. Study on evaluation of shale oil reservoir fracability based on well logging data volume. *Prog. Geophys.* **2018**, *33*, 603–612. (In Chinese with English abstract)
118. Wang, G.; Xiong, Z.; Zhang, J. The impact of lithology differences to shale fracturing. *J. Jilin Univ.* **2016**, *46*, 1080–1089. (In Chinese with English abstract)
119. Wang, Y.; Hou, B.; Wang, D.; Jia, Z. Features of fracture height propagation in cross-layer fracturing of shale oil reservoirs. *Pet. Explor. Dev.* **2021**, *48*, 469–479. [[CrossRef](#)]
120. Xu, D.; Hu, R.; Gao, W.; Xia, J. Effects of laminated structure on hydraulic fracture propagation in shale. *Pet. Explor. Dev.* **2015**, *42*, 573–579. [[CrossRef](#)]
121. Zhao, X.; Zhou, L.; Pu, X.; Jin, F.; Han, W.; Shi, Z.; Chen, C.; Jiang, W.; Guan, Q.; Xu, J.; et al. Theories, technologies and practices of lacustrine shale oil exploration and development: A case study of Paleogene Kongdian Formation in Cangdong sag, Bohai Bay Basin, China. *Pet. Explor. Dev.* **2022**, *49*, 707–718. [[CrossRef](#)]

Disclaimer/Publisher’s Note: The statements, opinions and data contained in all publications are solely those of the individual author(s) and contributor(s) and not of MDPI and/or the editor(s). MDPI and/or the editor(s) disclaim responsibility for any injury to people or property resulting from any ideas, methods, instructions or products referred to in the content.